DELFT UNIVERSITY OF TECHNOLOGY

DEPARTMENT OF AERONAUTICAL ENGINEERING

Report VTH-159

MATHEMATICAL MODEL OF EXTERNAL DISTURBANCES ACTING ON AN AIRCRAFT DURING AN ILS APPROACH AND LANDING

by

O. H. GERLACH

J. SCHURING

DELFT - THE NETHERLANDS

March 1970

DELFT UNIVERSITY OF TECHNOLOGY

DEPARTMENT OF AERONAUTICAL ENGINEERING

Report VTH-159

MATHEMATICAL MODEL OF EXTERNAL DISTURBANCES ACTING ON AN AIRCRAFT DURING AN ILS APPROACH AND LANDING

by

O. H. GERLACH

J. SCHURING

DELFT - THE NETHERLANDS

March 1970

Summary

This report presents a mathematical model of the external disturbances acting upon an aircraft during an I.L.S. approach and landing. Three different types of disturbances are distinguished: the wind, atmospheric turbulence and the noise contained in the I.L.S. signals. The model is thought to be applicable to altitudes between ground level and 450 m.

The basic material from which the model has been constructed, has been compiled from available literature.

1. Contents

2. Symbols

h	altitude
h_o	terrain factor
$i_{g.p}$	glide path current
i_ℓ	localizer current
I_x	polar moment of inertia about the X-axis
I_y	polar moment of inertia about the Y-axis
I_z	polar moment of inertia about the Z-axis
J_{xz}	product of inertia
L_i	scale of stochastic noise or turbulence, the index i indicating the variable concerned
L	aerodynamic moment about the aircraft's X-axis
m	aircraft's mass
M	aerodynamic moment about the aircraft's Y-axis
N	aerodynamic moment about the aircraft's Z-axis
p	power (in expression (4-1) for the wind speed)
p	rolling velocity about the aircraft's X-axis
q	pitching velocity about the aircraft's Y-axis
r	yawing velocity about the aircraft's Z-axis
r_l	distance from the aircraft's c.g. to the glide path antenna
R_T	terrain factor
$S_{g.p}$	sensitivity of the glide path system
S_ℓ	sensitivity of the localizer system

t	time
T	temperature
$\frac{dT}{dh}$	temperature lapse rate
u	component of $\vec{V}_a$ along the aircraft's X-axis
u_e	component of $\vec{V}_e$ along the aircraft's X-axis
u_{ee}	component of $\vec{V}_e$ along the earth-fixed X_e-axis
u_g	component of $\vec{V}_g$ along the aircraft's X-axis
u_w	component of $\vec{V}_w$ along the aircraft's X-axis
u_{we}	component of $\vec{V}_w$ along the earth-fixed X_e-axis
v	component of $\vec{V}_a$ along the aircraft's Y-axis
v_e	component of $\vec{V}_e$ along the aircraft's Y-axis
v_{ee}	component of $\vec{V}_e$ along the earth-fixed Y_e-axis
v_g	component of $\vec{V}_g$ along the aircraft's Y-axis
v_w	component of $\vec{V}_w$ along the aircraft's Y-axis
v_{we}	component of $\vec{V}_w$ along the earth-fixed Y_e-axis
$\vec{V}_a$	velocity of the aircraft's c.g. relative to the surrounding atmosphere
$\vec{V}_e$	velocity of the aircraft's c.g. relative to the earth
$\vec{V}_g$	turbulence velocity vector relative to the earth
$\vec{V}_w$	wind velocity vector relative to the earth
w	component of $\vec{V}_a$ along the aircraft's Z-axis
w_e	component of $\vec{V}_e$ along the aircraft's Z-axis
w_{ee}	component of $\vec{V}_e$ along the earth-fixed Z_e-axis
w_g	component of $\vec{V}_g$ along the aircraft's Z-axis
w_w	component of $\vec{V}_w$ along the aircraft's Z-axis

w_{we} component of $\vec{V}_w$ along the earth-fixed Z_e-axis

W aircraft's weight

x distance from the aircraft's c.g. to the glide path antenna along the runway centerline

x_e coordinate of the aircraft's c.g. along the earth-fixed X_e-axis

x_{th} distance to threshold

x_o distance from the localizer antenna to the threshold

X aerodynamic force along the aircraft's X-axis

y lateral deviation of an aircraft from the localizer reference plane

y_e coordinate of the aircraft's c.g. along the earth-fixed Y_e-axis

$y_{g.p}$ offset of the glide path antenna from the runway centerline

Y aerodynamic force along the aircraft's Y-axis

z_e coordinate of the aircraft's c.g. along the earth-fixed Z_e-axis

Z aerodynamic force along the aircraft's Z-axis

α angle of attack

β sideslip angle

ϑ angle of pitch

$\vartheta_{o_{g.p}}$ nominal glide path elevation angle

$\Delta\vartheta_{g.p}$ measured glide path error

σ_i standard deviation of a stochastic variable, the

	index i indicating the variable concerned
φ	angle of roll
Φ_i	power spectrum of a stochastic variable, the index i indicating the variable concerned
ψ	angle of yaw
Ψ	angle, defined in Fig. 9
ψ_w	direction of the wind relative to the earth-fixed X_e-axis
Ω	spatial circular frequency

Indices

g.p	glide path
ℓ	localizer

Systems of axes

In this report two systems of axes are used.

1. An aircraft-fixed right-handed reference-frame OXYZ. The origin O lies in the aircraft's centre of gravity, the positive X-axis lies in the plane of symmetry OXZ and points forward. The positive Y-axis points to the right, the positive Z-axis points downward.
2. An earth-fixed, right-handed reference-frame $O_e X_e Y_e Z_e$. The origin O_e has a fixed position on the surface of the earth. The X_e- and Y_e-axes lie in the horizontal plane, the positive Z_e-axis points downward.

Remark: the altitude of the aircraft is $h = - z_e$.

3. Introduction

The success of the approach and landing of an aircraft largely depends on the ability of the human or automatic pilot to suppress the effects of external disturbances acting upon the aircraft during the last phases of flight.

The problem of accurately following the nominal flight path is most acute under conditions of low visibility, when the approach is likely to be made using I.L.S. guidance signals.

This report endeavours to provide a mathematical description of the various disturbances to be considered in an I.L.S. approach and landing of an aircraft. The disturbances are thought to be mainly of two different origins: the motions of the air in the lower atmosphere and the noise in the I.L.S. signals.

When discussing the atmospheric disturbances, it is convenient to divide the motions of the air relative to the ground into two parts, usually indicated as the wind and atmospheric turbulence. Consequently the discussions in this report deal with three types of external disturbances:

a. wind,

b. atmospheric turbulence,

c. noise in the I.L.S. signals.

The data employed to construct the mathematical model for these external disturbances have been collected from the available literature. The resulting model is thought to be valid for conventional aircraft at altitudes between ground level and 450 m (1500 ft).

It should be remarked that the various disturbances are grouped together since they all originate from sources external to the aircraft. Nevertheless, they influence the motions of the aircraft in quite dissimilar ways, see Fig. 1.

The wind is seen to primarily influence the motion of the aircraft relative to the ground. Atmospheric turbulence acts directly on the aircraft through aerodynamic forces and moments which have been

calculated at several places in the literature, e.g. see Refs. 4 and 5. The noise in the I.L.S. signals enters the aircraft through the on board I.L.S. equipment. Disturbances of the latter type have an influence on the aircraft's behaviour only via the human or the automatic pilot.

4. Mathematical model of the wind

4.1 General

In the context of this report the wind velocity vector $\vec{V}_w$ is defined as the average over a certain area in the horizontal plane at a certain height above the terrain and over a certain time interval, of the velocity vector of the air relative to the ground. The time interval over which the average is to be taken, should be chosen much larger than the interval during which the aircraft is affected by the air velocity at a certain point in space, yet it is to be taken small enough relative to the time scale on which changes in the general atmospheric conditions occur.

It is assumed that the wind velocity vector $\vec{V}_w$ as just defined has no vertical component at the low altitudes above essentially level ground to be considered in this report. In the horizontal plane the wind velocity vector $\vec{V}_w$ is described by a magnitude V_w (the wind speed) and by the wind direction, ψ_w, or by its components u_{we} and v_{we} along the two orthogonal X_e- and Y_e-axes. Either combination of two elements of the wind vector will depend on the altitude above the ground and on the stability of the atmosphere as expressed by the temperature lapse rate, $\frac{dT}{dh}$.

4.2 Wind speed as a function of height

Due to the friction of the air over the ground, wind speed decreases markedly with decreasing height in the lower layers of the

atmosphere. The resulting wind profile depends in principle on the type of terrain and on the stability of the atmosphere, see Ref. 2. From the data given in Ref. 2, it appears that likely variations in the type of terrain have an influence on the wind profile well within the scatter of the experimental data.

According to Ref. 2, a logarithmic law describes the wind profile well for adiabatic and unstable conditions, where the lapse rate $\frac{dT}{dh}$ is greater than $0{,}01\,^{\circ}C/m$. A power law appears to be more suitable for stable conditions, where $\frac{dT}{dh} < 0{,}01\,^{\circ}C/m$. Taking the wind at 9,15 m (30 ft) as a reference value and assuming V_w to be constant above 300 m, the following expressions for the wind speed result.

a. $0 < \frac{dT}{dh} < 0{,}01\,^{\circ}C/m$

$$V_w = V_{w_{9,15}} \cdot \frac{h^p - h_o^p}{9,15^p - h_o^p} \qquad 0 < h < 300 \text{ m}$$

where: $h_o = 0{,}03$ m

and: $p = 0{,}43 - 27 \cdot \frac{dT}{dh}$

$$V_w = V_{w_{300}} \qquad h \geqslant 300 \text{ m}$$

(4-1)

b. $\frac{dT}{dh} \geqslant 0{,}01\,^{\circ}C/m$

$$V_w = V_{w_{9,15}} \left(\frac{\log h}{2{,}477} + 0{,}620\right) \qquad 0 < h < 300 \text{ m}$$

$$V_w = V_{w_{300}} = 1{,}62\, V_{w_{9,15}} \qquad h \geqslant 300 \text{ m}$$

(4-2)

These wind profiles are shown in Fig. 2.

4.3 Wind direction as a function of height

In the lowest layers of the atmosphere a variation of the wind direction occurs, due to the friction of the air over the ground.

Such shifts in wind direction are termed veering if the wind turns clockwise and barking if the wind turns counterclockwise with increasing height. Data presented in Table 5.5 of Ref. 6 show that the wind veers with height on the average about $0{,}04^{o}$/m, to a height of some 900 m (3000 ft) over coastal plains on the Northern Hemisphere.

4.4 Wind as a function of atmospheric conditions

Clearly the wind speed and direction are strongly related to the prevailing atmospheric conditions. Since the particular location of the airfield under consideration also has a very marked influence on the wind to be expected under given atmospheric conditions, no attempt has been made in this report to find a general expression for the wind as a function of those atmospheric conditions. Rather it is assumed that the wind - at some reference height , e.g. 9,15 m - be given as an independent variable when describing the external disturbances acting on the aircraft during approach and landing.

5. Mathematical model of atmospheric turbulence

5.1 General

Earlier in this report the motion of the air relative to the ground has been divided into two parts : the wind and atmospheric turbulence. Bearing in mind the definition of the wind given in 4.1, the turbulence velocity vector $\vec{V}_g$ can now be defined as the momentary difference between the velocity of an air particle relative to the earth at a certain instant in time and at a certain height, and the

wind velocity vector $\vec{V}_w$ at that time and altitude.

Atmospheric turbulence has been studied at length in the literature, e.g. Ref. 3. In this report use is made mainly of the data given in Ref. 1. The main reason for this choice has been the fact that these data have been collected from an extensive survey of other publications, and moreover they have been presented in a form well suited for the present purpose.

It is general practice to think of atmospheric turbulence as a stochastic process. This permits describing the phenomenon in terms of power spectral density functions. In line with Ref. 1, the approach adopted here to express the turbulence in quantitive terms is a semi-empirical one. The structure of the expressions giving the spectral density functions of the components u_g, v_g and w_g of $\vec{V}_g$ have been taken from theoretical work on homogeneous isentropic turbulence.

The spectra to be used are those due to Dryden, see Ref. 1:

$$\Phi_{u_g}(\Omega) = \sigma_{u_g}^2 \cdot \frac{2L_u}{\pi} \cdot \frac{1}{1+\Omega^2 L_u^2}$$

$$\Phi_{v_g}(\Omega) = \sigma_{v_g}^2 \cdot \frac{L_v}{\pi} \cdot \frac{1+3\Omega^2 L_v^2}{(1+\Omega^2 L_v^2)^2} \qquad \Omega \text{ in rad/m}$$

$$\Phi_{w_g}(\Omega) = \sigma_{w_g}^2 \cdot \frac{L_w}{\pi} \cdot \frac{1+3\Omega^2 L_w^2}{(1+\Omega^2 L_w^2)^2}$$

The intensity of the turbulence is expressed by the variances:

$$\sigma_i^2 = \int_0^\infty \Phi_i(\Omega) \cdot d\Omega \qquad i = u_g, v_g, w_g$$

In isentropic turbulence no differences exist between the variances $\sigma_{u_g}^2$, $\sigma_{v_g}^2$ and $\sigma_{w_g}^2$, also the three scales L_u, L_v and L_w are identical.

The quantitative values of the variances and the scales of the turbulence actually to be inserted in the above power spectra are based on experimental data, see Ref. 1. As might be expected, these experimental data show the variances and scales to be functions of height. The vertical component w_g behaves different from the horizontal components u_g and v_g. As a consequence, turbulence at the low altitudes considered is neither homogeneous nor isentropic.

The following paragraphs present the numerical data proposed for the mathematical model of atmosphere turbulence at low altitude. Following Ref. 1, the intensity and the scale of the vertical component w_g are described first, then the corresponding characteristics of the two horizontal components u_g and v_g are related to those of w_g.

5.2 Intensity of the turbulence

5.2.1 Vertical component, w_g

The standard deviation of vertical gust velocity σ_{w_g} is presented in Fig. 3, see also Fig. 1 of Ref. 1. Clearly, σ_{w_g} depends on a terrain factor R_T, the wind speed V_w, the height and also on the stability of the atmosphere as expressed by the temperature lapse rate.

The terrain factor to be used can be chosen from the following Table 1.

Type of terrain	R_T
Ocean, desert	1
Farmland	1,1
Forest, swamp	1,15
Low mountains	1,3
High mountains	1,4

Table 1: Terrain factor R_T

In many cases of practical interest it may be assumed that:

$$R_T = 1,1$$

When calculating σ_{w_g} at a certain altitude, the wind at that altitude has to be used in Fig. 3. Assuming the wind speed to increase with altitude according to (4-1) and (4-2) given in 4.2, a relation between σ_{w_g} and altitude results as depicted in Fig. 4 for $R_T = 1,1$. In this Figure a wind speed at 9,15 m and a temperature lapse rate are needed to find σ_{w_g} at any altitude between 0 and 450 m.

5.2.2 Horizontal components, u_g and v_g

As was mentioned in 5.1, σ_{u_g} and σ_{v_g} are equal to σ_{w_g} in isentropic turbulence. According to Ref. 1, such experimental data as exist, lead to the following expressions for σ_{u_g} and σ_{v_g}.

a. Stable and neutral atmosphere, $0 < \frac{dT}{dh} \leq 0{,}01\,^{\circ}C/m$

$$\frac{\sigma_{u_g}}{\sigma_{w_g}} = 3 \quad ; \quad \frac{\sigma_{v_g}}{\sigma_{w_g}} = 2 \qquad 0 \leq h < 15$$

$$\frac{\sigma_{u_g}}{\sigma_{w_g}} = \frac{\sigma_{v_g}}{\sigma_{w_g}} = 1{,}2 - 0{,}00056\,h \qquad 15 \leq h < 360 \qquad h \text{ in m}$$

$$\frac{\sigma_{u_g}}{\sigma_{w_g}} = \frac{\sigma_{v_g}}{\sigma_{w_g}} = 1 \qquad h > 360$$

b. Unstable atmosphere, $\frac{dT}{dh} > 0{,}01\,^{\circ}C/m$

$$\frac{\sigma_{u_g}}{\sigma_{w_g}} = 3 \quad ; \quad \frac{\sigma_{v_g}}{\sigma_{w_g}} = 2 \qquad 0 \leq h < 15$$

$$\frac{\sigma_{u_g}}{\sigma_{w_g}} = \frac{\sigma_{v_g}}{\sigma_{w_g}} = 1{,}3 - 0{,}0019\,h \qquad 15 \leq h < 160 \qquad h \text{ in m}$$

$$\frac{\sigma_{u_g}}{\sigma_{w_g}} = \frac{\sigma_{v_g}}{\sigma_{w_g}} = 1 \qquad h > 160$$

In view of the considerable scatter in the data on which these expressions are based, it seems to be justified to simplify the model by combining the two sets into the following relations for all stability conditions of the atmosphere.

c. All stability conditions of the atmosphere

$$\frac{\sigma_{u_g}}{\sigma_{w_g}} = \frac{\sigma_{v_g}}{\sigma_{w_g}} = 2{,}5 \qquad 0 \leqslant h < 15$$

$$\frac{\sigma_{u_g}}{\sigma_{w_g}} = \frac{\sigma_{v_g}}{\sigma_{w_g}} = 1{,}25 - 0{,}001\,h \qquad 15 \leqslant h < 250 \qquad h \text{ in m}$$

$$\frac{\sigma_{u_g}}{\sigma_{w_g}} = \frac{\sigma_{v_g}}{\sigma_{w_g}} = 1 \qquad h > 250$$

The resulting ratios of the standard deviations as a function of altitude are given in Fig. 5.

5.3 Scale of the turbulence

5.3.1 Vertical component, w_g

The information available on L_w has been presented in Fig. 6, see also Fig. 2 of Ref. 1. For a given temperature lapse rate, L_w can be read directly as a function of altitude.

5.3.2 Horizontal components, u_g and v_g

The isentropic condition:

$$L_u = L_v = L_w$$

does not seem to hold too well at low altitudes. Based on Ref. 1,

the following relation between L_u, L_v and L_w is proposed for all stability conditions of the atmosphere:

$$\frac{L_u}{L_w} = \frac{L_v}{L_w} = 1{,}27 \qquad 0 \leqslant h < 15$$

$$\frac{L_u}{L_w} = \frac{L_v}{L_w} = 1{,}3 - 0{,}002\,h \qquad 15 \leqslant h < 150 \qquad h \text{ in m}$$

$$\frac{L_u}{L_w} = \frac{L_v}{L_w} = 1 \qquad h > 150$$

These ratios are plotted in Fig. 7 against altitude.

5.4 Concluding remark

From the foregoing it can be concluded that the entire structure of the wind and the atmospheric turbulence during approach and landing can be described, according to the model just presented, by giving:

a. the wind speed and direction at some reference height, e.g. 9,15 m
b. the temperature lapse rate of the lower atmosphere
c. a terrain factor

Since the likely variations in the terrain factor appear to be relatively small, the external distrubances due to the atmosphere, acting on the aircraft at a certain altitude, are seen to depend primarily on the wind speed and on the stability of the atmosphere.

6. Mathematical model of the I.L.S. signals

6.1 General

Before dealing with the noise and other disturbances contained in the I.L.S. signals, it may be useful first to give a very brief description of the nominal I.L.S. signals. A more detailed description of the Instrument Landing System can be found e.g. in Ref. 7. Requirements to be satisfied by an I.L.S. installation have been set forth by I.C.A.O., see Refs. 8 and 9. The ground based part of the I.L.S. installation of interest in this discussion is sketched in Fig. 8.

I.L.S. provides guidance to the approaching aircraft in two planes. The localizer signal, emitted by the localizer antenna situated beyond the far end of the runway, provides a left or right indication relative to the vertical localizer reference plane passing through the runway center line. The glide path signal, emitted by the glide path antenna located some 300 m beyond the runway threshold, provides an up or down indication relative to the glide path reference plane. The latter plane passes through the glide path antenna. Its intersection with the localizer plane is the nominal glide path to be followed by the aircraft during its final approach. The angle $\theta_{o_{g.p}}$ between the nominal glide path and the horizontal is set at some angle between 2 and 4^{o}. In many cases an angle of $2{,}5^{o}$ is used, this being the preferred I.L.S. glide path angle according to 3.1.4.1.2.1 of Ref. 8.

The localizer and glide path signals are received on board the approaching aircraft. They are displayed in a suitable form to the pilot and may be fed directly to the automatic pilot as well.

Ideally, the two I.L.S. reference planes should be perfectly flat planes. Due to interference effects caused by buildings, high tension cables, taxiing or overflying aircraft etc., the reference planes become distorted. Most of these distortions may be interpreted

as noise superimposed on the nominal I.L.S. signals.

Usually the nominal I.L.S.signals on board the aircraft are expressed in terms of the direct currents (in μA) supplied to the pilot's I.L.S. indicator.

An I.L.S. installation is said to be belong to a certain Performance Category, according to the meteorological conditions under which the installation is to be used.

The meteorological conditions are summarized in the following Table 2.

Approach Category	Meteorological conditions	
	Cloud base, m	Runway Visual Range, m
I	60	800
II	30	400
IIIa	0	200
IIIb	0	50
IIIc	0	0

Table 2: Definition of meteorological conditions for approach and landing

An I.L.S. installation of Performance Category I is intended to provide guidance down to an altitude of 60 m, an installation of Performance Category II provides guidance down to 30 m, whereas an installation of Performance Category III should provide guidance to the landing aircraft, down to the surface of the runway, see 3.1.1 of Ref. 8.

6.2 The nominal signals

6.2.1 The nominal localizer component

Due to the characteristics of the signals emitted from the localizer antenna, points of constant (nominal) localizer current lie in vertical planes passing through the antenna, see Fig. 9. The magnitude of the localizer current i_ℓ depends on the angle Ψ. The current will be:

$$i_\ell = S_\ell \cdot \Psi$$

where i_ℓ is measured in μA and S_ℓ is the sensitivity of the system. According to 3.1.3.5.5.1 of Ref. 8 and 2.2.2 of Ref. 9, S_ℓ has to satisfy the following relation:

$$S_\ell = 1{,}40 \cdot x_o \qquad \mu A/rad$$

where x_o is the distance from the localizer antenna to the runway threshold (in m). Due to this condition, a fixed relation exists between the localizer current as presented to the pilot, and the lateral deviation of the aircraft when passing over the runway threshold, see Fig. 9. If the aircraft has a lateral deviation y relative to the localizer reference plane:

$$y = 0{,}71 i_\ell$$

y in m, i_ℓ in μA

The maximum permissible deviations of the localizer sensitivity S_ℓ from its nominal value, as given in 3.1.3.5.5.2 of Ref. 8, are summarized in Table 3.

Performance Category	Maximum deviation from nominal sensitivity
I	± 17 °/o
II	± 17 °/o (± 10°/o where practicable)
III	± 10 °/o

Table 3: Maximum permissible deviations from nominal localizer sensitivity

The localizer plane should be adjusted such, that it deviates not more than a specified distance from the runway centerline at the runway threshold. According to 3.1.3.5.4 and 3.3.3.5.4.1 of Ref. 8 these distances are as indicated in Table 4.

Performance Category	Maximum deviation, m
I	± 10,5
II	± 7,5 (± 4,5 for new installations)
III	± 3

Table 4: Maximum deviation of localizer plane from runway centerline at runway threshold

The maximum value of the localizer current i_ℓ has been limited in 2.2.2 of Ref. 9 to ± 150μA.

6.2.2 The nominal glide path component

The signals emitted from the glide path antenna cause the glide path reference plane actually to be a cone with a vertical axis, having its apex in the glide path antenna. This would not become readily apparent if the antenna were situated on the runway centerline. In order to prevent the aircraft from colliding with the antenna, however, the latter is positioned some 120 to 150 m away from the centerline. Consequently, the line of intersection of the localizer reference plane and the glide path reference plane is a hyperbola a small distance above the idealized straight glide path reference plane, see Fig. 10. The distance varies along the runway center line from about 2 m at the runway threshold to some 7,5 m abeam the glide path antenna.

The I.L.S. indicator on board the aircraft provides a measure of the aircraft's deviation from the glide-path. Since points in space providing a constant glide path current to the instrument lie on a cone, as in Fig. 10, the measured glide path error $\Delta\varphi_{g.p.}$ amounts to, see Fig. 11:

$$\Delta\varphi_{g.p.} = \frac{h}{r_1} - \varphi_{o_{g.p.}}$$

where $\varphi_{o_{g.p.}}$ is the nominal glide path elevation angle,

$$r_1 = \sqrt{x^2 + (y_{g.p.} - y)^2}$$

and x,y and $y_{g.p.}$ are as indicated in Fig. 11.

The glide path current $i_{g.p.}$ corresponding to $\Delta\varphi_{g.p.}$ is:

$$i_{g.p.} = S_{g.p.} \cdot \Delta\varphi_{g.p.}$$

where $i_{g.p.}$ is expressed in μA and $\Delta\Theta_{g.p}$ in rad.

The sensitivity $S_{g.p.}$ follows from 3.1.4.6 of Ref. 8 and 2.2.3 of Ref. 9:

$$S_{g.p.} = \frac{625}{\Theta_{o_{g.p.}}} \quad \frac{\mu A}{rad}$$

$\Theta_{o_{g.p.}}$ in rad

The allowable tolerances of this nominal value of the sensitivity, as given in 3.1.4.6.6/7/8 of Ref. 8, are as presented in Table 5.

Performance Category	Maximum deviation
I	$\pm$ 25 °/o
II	$\pm$ 20 °/o
III	$\pm$ 15 °/o

Table 5: Maximum deviation from nominal glide path sensitivity

According to 3.14.1.2.2 of Ref. 8, the actual glide path angle shall lie between the limits indicated in Table 6.

Performance Category	Maximum deviation
I	$\pm$ 0,075 $\Theta_{o_{g.p.}}$
II	$\pm$ 0,075 $\Theta_{o_{g.p.}}$
III	$\pm$ 0,04 $\Theta_{o_{g.p.}}$

Table 6: Maximum deviations of nominal glide path angle $\Theta_{o_{g.p.}}$

The nominal glide path shall pass over the runway threshold at 15 m $\pm$ 3 m according to 3.1.4.1.4.

For all Performance Categories, the maximum value of the glide path current $i_{g.p.}$ has been limited to $\pm$ 150μA, according to 2.2.3 of Ref. 9.

6.3 The noise signals

6.3.1 General

From measurements presented in Ref. 10 it appears that localizer and glide path noises - apart from incidental disturbances caused e.g. by overflying aircraft - can be approximated by stochastic signals having rather simple power spectral density functions. Since the I.L.S. noise greatly influences the accuracy with which an approach can be flown, I.C.A.O. has set upper limits to the allowable standard deviations of the noise. No limitations have been set so far on the allowable shape of the power spectra of the noise.

The disturbances caused by an aircraft flying in the vicinity of the localizer antenna will be discussed in 6.4.

6.3.2 Localizer noise component

According to Ref. 10 the power spectral density function of the localizer noise can be approximated by:

$$\Phi_{\ell}(\Omega) = \sigma_{\ell}^{2} \cdot \frac{2L_{\ell}}{\pi} \cdot \frac{1}{1 + \Omega^{2} L_{\ell}^{2}}$$

Ω in rad/m

where the ''scale'' of the localizer noise is taken at approximately:

$$L_{\ell} = 130 \text{ m}$$

The intensity of the noise, as expressed by σ_{ℓ} in μA, has been limited in 3.1.3.4.1 of Ref. 8, as given in Table 7. x_{th} indicates the distance of the approaching aircraft to the runway threshold.

Performance Category	Distance to threshold, x_{th} in m		
	$x_{th} > 7410$	$7410 > x_{th} > 1050$	$x_{th} < 1050$
I	15μA	$6,25 + 1,18.10^{-3} x_{th}$	7,5μA
II	15μA	$0,44 + 1,96.10^{-3} x_{th}$	2,5μA
III	15μA	$0,44 + 1,96.10^{-3} x_{th}$	2,5μA

Table 7: Maximum allowable localizer noise, σ_{ℓ}

These relations are shown in Fig. 12.

6.3.3 Glide path noise component

The power spectral density function of the glide path noise appears to be somewhat similar to that of the localizer noise,

according to Refs. 10 and 11.

$$\Phi_{g.p.}(\Omega) = \sigma^2_{g.p.} \cdot \frac{2L_{g.p.}}{\pi} \cdot \frac{1}{1 + \Omega^2 . L^2_{g.p.}}$$

Ω in rad/m

where the ''scale'' of the glide path noise can be approximated by:

$$L_{g.p.} = 85 \text{ m}$$

The intensity of the glide path noise, again expressed by $\sigma_{g.p.}$ in μA, has been limited in 3.1.4.4.1 and 3.1.4.4.2 of Ref. 8 to the values presented in Table 8.

Performance Category	Distance to threshold, x_{th}, in m		
	$x_{th} > 7410$	$7410 > x_{th} > 1050$	$x_{th} < 1050$
I	15μA	15μA	15μA
II	15μA	$9,20+0,785.10^{-3}.x_{th}$	10μA
III	15μA	$9,20+0,785.10^{-3}.x_{th}$	10μA

Table 8: Maximum allowable glide path noise, $\sigma_{g.p.}$

These relations are also shown in Fig. 12.

6.4 Disturbances in the localizer signal due to overflying aircraft

Apart from the stochastic noise in the I.L.S. signals discussed in the previous paragraphs, yet another type of disturbances peculiar to the I.L.S. localizer has to be considered.

When an aircraft flies in the vicinity of the localizer antenna, e.g. when taking off, part of the electromagnetic energy radiated from the antenna is reflected by the skin of the overflying aircraft. Another aircraft flying at the same time along the approach path of the I.L.S. installation may experience an erroneous Localizer signal due to the reflected energy. The interference signal may cause quite significant deviations from the intended approach path.

Although this type of disturbances can be quite severe, not much quantitative evidence on its characteristics exists. Some data can be found, however, in Ref. 12. A number of such disturbances, as derived from in-flight measurements, presented in Ref. 12, are shown in Fig. 13. A more detailed discussion on this particular type of disturbances will also be found in Ref. 12.

Following a suggestion made in that report, the disturbance in the localizer signal due to interference from an overflying aircraft is approximated by a swept frequency sinusoidal oscillation having an approximately exponential rate of change of frequency. The duration of the disturbance may be between 10 and 20 seconds. In the first half of that period the interference frequency is swept from zero to 1,0 Hz, and in the second half from 1,0 to 10,0 Hz. The amplitude of the disturbance increases linearly with time from zero to a maximum of 75 μA peak to peak in the first half of the disturbance period, remaining approximately constant thereafter. The starting phase of the oscillation may be chosen at random. Fig. 14 shows some of the possible disturbances according to the given description.

Using this model of interference from an overflying aircraft, non-sinusoidal and asymmetric characteristics of the real interferences are neglected. It is felt that insufficient data are available at the present time to warrant their inclusion into a realistic model of the disturbances.

It has to be borne in mind, that the quantitative evidence on which the description of disturbances of this kind has been based, is due to measurements with one type of aircraft only, a Vickers

''Varsity''. Different and in particular larger aircraft taking off over the localizer antenna may cause even more severe disturbances in the localizer signal.

Under the present regulations of Air Traffic Control, an aircraft approaching to land may experience the disturbance due to another aircraft taking off over the localizer antenna at any instant during the approach. It seems reasonable to assume that if such a disturbance does occur at all, it will happen not more than once during one approach and landing.

7. References

1. Pritchard, F.E.: A statistical model of atmospheric turbulence and a review of the assumptions necessary for its use. AGARD Conference Proceedings no. 17 Part II. AGARD, Paris, 1966.

2. Lappe,U. O.: A low altitude turbulence model for estimating gust loads on aircraft, AIAA Paper no. 65-14, 1965.

3. Lumley, J.L. and H.A. Panofsky: The structure of atmospheric turbulence. John Wiley and Sons, New York, 1964.

4. Gerlach, O.H.: Calculation of the response of an aircraft to random atmospheric turbulence. Part I: Symmetric motions. Report VTH-138, Delft University of Technology, Department of Aeronautical Engineering, Delft, 1966.

5. Gerlach, O.H. and M. Baarspul: Calculation of the response of an aircraft to random atmospheric turbulence, Part II: Asymmetric motions. Report VTH-139. Delft University of Technology, Department of Aeronautical Engineering, Delft, 1968.

6. Anon.: Handbook of geophysics, Revised edition. U.S.A.F. Air Research and Development Command, McMillan Book Cy., New York, 1960.

7. Worthington, G.D.P.: Airline instrument flying, Pitman and Sons

Ltd., London, 1968.

8. Anon.: International standards and recommended practices, Annex 10, Volume I, Part I: Equipment and systems. I.C.A.O., Montreal, 1968.

9. Anon.: International standards and recommended practices, Annex 10, Volume I, Attachment C to Part I. I.C.A.O., Montreal, 1968.

10. Weir, D.H.: Compilation and analysis of flight control system command inputs. Technical Report AFFDL-TR-65-119, Air Force Flight Dynamics Laboratory, Wright-Patterson A.F. Base, Ohio, 1966.

11. McRuer, D. a.o.: A systems analysis theory for displays in manual control. STI Technical Report 163-1, Systems Technology, Inc. Hawthorne, California, 1968.

12. Hughes, N.H.: The effects on automatic landing lateral performance of interference to the I.L.S. localizer by reflection from an aircraft taking-off. R.A.E. Technical Report 68156, Farnborough, 1968.

13. Etkin, B: Dynamics of flight. John Wiley and Sons, Inc., New York, 1959.

8. Appendix. Influence of a variable wind on the motions of an aircraft

When deriving the equations of motion of an aircraft, the simplifying assumption is often made that the atmosphere is at rest or has a constant velocity relative to the earth. In many practical applications of the equations, however, such an assumption is not acceptable.

In their usual form the equations of motion of an aircraft read, e.g. see Ref. 13:

$$
\begin{aligned}
-W\sin\Theta \qquad\qquad + X &= m\,(\dot{u} + qw - rv)\\
W\cos\Theta\sin\Phi + Y &= m\,(\dot{v} + ru - pw)\\
W\cos\Theta\sin\Phi + Z &= m\,(\dot{w} + pv - qu)
\end{aligned}
\qquad (8\text{-}1)
$$

$$
\begin{aligned}
L &= I_x\dot{p} + (I_z - I_y)qr - J_{xz}(\dot{r} + pq)\\
M &= I_y\dot{q} + (I_x - I_z)rp + J_{xz}(p^2 - q^2)\\
N &= I_z\dot{r} + (I_y - I_x)pq - J_{xz}(\dot{p} - rq)
\end{aligned}
\qquad (8\text{-}2)
$$

$$
\begin{aligned}
\dot{\Psi} &= q\,\frac{\sin\Phi}{\cos\Theta} + r\,\frac{\cos\Phi}{\cos\Theta}\\
\dot{\Theta} &= q\cos\Phi - r\sin\Phi\\
\dot{\Phi} &= p + q\sin\Phi\,\mathrm{tg}\,\Theta + r\cos\Phi\,\mathrm{tg}\,\Theta
\end{aligned}
\qquad (8\text{-}3)
$$

The first three equations (8-1) are true only, if u, v and w are the components of the translational velocity of the aircraft's c.g. relative to a non-rotating system of reference axes having a constant translational speed in inertial space.

If the wind velocity vector $\vec{V}_w$ is constant, the atmospheric air has such a constant speed relative to inertial space, assuming no turbulence. In such a case it is indeed admissable to use in the equations (8-1) the velocity $\vec{V}_a$ of the aircraft's c.g. relative to the surrounding atmosphere. The advantage of fixing the reference axes to the atmosphere lies in the fact that then the airspeed $\vec{V}_a$ is derived from the equations (8-1), while the same velocity is needed as well to calculate the aerodynamic forces X, Y, Z in (8-1) and the aerodynamic moments L, M, N in (8-2).

A complication arises, however, if the wind velocity $\vec{V}_w$ is not constant during the time interval over which the aircraft's motions

are studied. This situation may occur during the approach and landing of an aircraft, as discussed in Section 4. Then the system of reference axes cannot be fixed to the surrounding atmosphere.

The subsequent part of this Section indicates how the aircraft's motions can be described in such a case. In accordance with Section 4 it is assumed that the variable wind velocity vector $\vec{V}_w$ has no vertical component. Furthermore, atmospheric turbulence is not considered, since its effects can be described separately, e.g. see Refs. 4 and 5.

The system of reference axes will be the earth-fixed axes, as defined in Section 2. As a consequence, in the equations of motion (8-1) appear the components u_e, v_e, w_e of the velocity vector $\vec{V}_e$ relative to the earth, where u_e, v_e, w_e are the components of $\vec{V}_e$ along the aircraft's body axes. The equations of motion (8-1) now become:

$$\begin{aligned} -W \sin\Theta \qquad\qquad + X &= m(\dot{u}_e + q\, w_e - r\, v_e) \\ W \cos\Theta \sin\varphi + Y &= m(\dot{v}_e + r\, u_e - p\, w_e) \\ W \cos\Theta \cos\varphi + Z &= m(\dot{w}_e + p\, v_e - q\, u_e) \end{aligned} \tag{8-4}$$

The results of an integration of these equations are the components u_e, v_e, w_e of $\vec{V}_e$. However, the aerodynamic forces X, Y, Z in (8-4) and the moments L, M, N in (8-2) are functions of the velocity vector $\vec{V}_a$ of the aircraft's c.g. relative to the surrounding atmosphere. The components of $\vec{V}_a$ are u, v, w as in (8-1). The difference between $\vec{V}_e$ and $\vec{V}_a$ is, of course, the wind velocity vector $\vec{V}_w$.

$$\vec{V}_a = \vec{V}_e - \vec{V}_w \tag{8-5}$$

Designating the components of the wind vector $\vec{V}_w$ along the aircraft's body axes by u_w, v_w, w_w, the three scalar expressions equivalent to (8-5) are:

$$\begin{aligned} u &= u_e - u_w \\ v &= v_e - v_w \\ w &= w_e - w_w \end{aligned} \tag{8-6}$$

The components u_w, v_w, w_w of $\vec{V}_w$ are obtained from given values of u_{we}, v_{we}, w_{we} (= 0) along the earth-fixed axes. To this end, subsequent rotations of axes through the angles ψ, ϑ and φ from the earth-fixed reference system to the attitude of the aircraft's body axes are applied, Fig. 15. The transformation matrices expressing each of these three rotations separately are:

$$[\psi] = \begin{bmatrix} \cos\psi & \sin\psi & 0 \\ -\sin\psi & \cos\psi & 0 \\ 0 & 0 & 1 \end{bmatrix} \tag{8-7}$$

$$[\vartheta] = \begin{bmatrix} \cos\vartheta & 0 & -\sin\vartheta \\ 0 & 1 & 0 \\ \sin\vartheta & 0 & \cos\vartheta \end{bmatrix} \tag{8-8}$$

$$[\varphi] = \begin{bmatrix} 1 & 0 & 0 \\ 0 & \cos\varphi & \sin\varphi \\ 0 & -\sin\varphi & \cos\varphi \end{bmatrix} \tag{8-9}$$

The resulting transformation of u_{we}, v_{we}, w_{we} (= 0) in the earth-fixed reference system to u_w, v_w, w_w along the aircraft's body axes is:

$$\begin{bmatrix} u_w \\ v_w \\ w_w \end{bmatrix} = [\varphi] \cdot [\Omega] \cdot [\psi] \cdot \begin{bmatrix} u_{we} \\ v_{we} \\ 0 \end{bmatrix}$$

or:

$$\begin{bmatrix} u_w \\ v_w \\ w_w \end{bmatrix} = \begin{bmatrix} \cos\psi.\cos\Omega & \sin\psi.\cos\Omega & -\sin\Omega \\ \cos\psi.\sin\Omega\sin\varphi - \sin\psi.\cos\varphi & \sin\psi.\sin\Omega\sin\varphi + \cos\psi.\cos\varphi & \cos\Omega\sin\varphi \\ \cos\psi.\sin\Omega\cos\varphi + \sin\psi.\sin\varphi & \sin\psi.\sin\Omega\cos\varphi - \cos\psi.\sin\varphi & \cos\Omega\cos\varphi \end{bmatrix} \cdot \begin{bmatrix} u_{we} \\ v_{we} \\ 0 \end{bmatrix}$$

Usually the given wind velocity vector $\vec{V}_w$ is expressed by the wind speed V_w and its direction ψ_w relative to the earth-fixed axes, rather than by its components u_{we} and v_{we}, see Section 4. When describing the wind direction by ψ_w some care has to be taken, see Fig. 16, since:

$$u_{we} = V_w . \cos(\psi_w - 180^o)$$
$$v_{we} = V_w . \sin(\psi_w - 180^o)$$

This means, for example, that a wind vector along the positive X_e- axis is indicated by an angle $\psi_w = 180^o$.

If V_w and ψ_w are given, u_w, v_w and w_w can be derived from (8-10) by equating u_{we} to V_w and V_{we} to zero and by replacing ψ by $\psi - (\psi_w - 180^o)$, see Fig. 17. The result is:

$$\begin{bmatrix} u_w \\ v_w \\ w_w \end{bmatrix} = \begin{bmatrix} -\cos(\psi_w - \psi).\cos\Omega \\ -\cos(\psi_w - \psi)\sin\Omega\sin\varphi - \sin(\psi_w - \psi)\cos\varphi \\ -\cos(\psi_w - \psi)\sin\Omega\cos\varphi + \sin(\psi_w - \psi)\sin\varphi \end{bmatrix} .V_w \qquad (8\text{-}11)$$

Using (8-10) or (8-11), u_w, v_w and w_w can now be calculated from a given V_w. The components u, v, w of V_a are found from (8-6) if u_e, v_e and w_e in (8-6) have been obtained by integrating the equations of motion (8-4), (8-2) and (8-3).

The magnitude V_a of V_a is:

$$V_a = \sqrt{u^2 + v^2 + w^2}$$

The angle of attack α is:

$$\alpha = \text{arctg} \frac{w}{u}$$

and the sideslip angle β is:

$$\beta = \arcsin \frac{v}{V_a}$$

These three variables V_a, α and β are required to calculate the aerodynamic forces X, Z in (8-4) and the aerodynamic moments L, M, N in (8-2).

If the translations of the aircraft's c.g. relative to the earth need to be known, the components u_{ee}, v_{ee}, w_{ee} of V_e along the earth-fixed axes have to be calculated. These u_{ee}, v_{ee}, w_{ee}, are computed from the known u_e, v_e, w_e along the aircraft's body axes. Subsequent rotations of axes through the angles $-\varphi$, $-\Theta$, - ,bring the aircraft's body axes into the attitude of the earth-fixed axes, see Fig. 15. The three transformation matrices expressing each of these rotations are derived directly from (8-7), (8-8) and (8-9), either by inversion or, more simply, by replacing sin by -sin. The resulting total transformation is:

$$\begin{bmatrix} u_{ee} \\ v_{ee} \\ w_{ee} \end{bmatrix} = \left[-\psi\right] \cdot \left[-\theta\right] \cdot \left[-\varphi\right] \cdot \begin{bmatrix} u_e \\ v_e \\ w_e \end{bmatrix}$$

or:

$$\begin{bmatrix} u_{ee} \\ v_{ee} \\ w_{ee} \end{bmatrix} = \begin{bmatrix} \cos\psi.\cos\theta & -\sin\psi.\cos\varphi+\cos\psi.\sin\theta\sin\varphi & \sin\psi.\sin\varphi+\cos\psi.\sin\theta\cos\varphi \\ \sin\psi.\cos\theta & \cos\psi.\cos\varphi+\sin\psi.\sin\theta\sin\varphi & -\cos\psi.\sin\varphi+\sin\psi.\sin\theta\cos\varphi \\ -\sin\theta & \cos\theta\sin\varphi & \cos\theta\cos\varphi \end{bmatrix} \cdot \begin{bmatrix} u_e \\ v_e \\ w_e \end{bmatrix}$$

Once the components u_{ee}, v_{ee}, w_{ee} of $\vec{V}_e$ along the earth-fixed axes are known, the coordinates x_e, y_e, z_e in the same system of axes are obtained by integration:

$$x_e = x_e(0) + \int_0^t u_{ee}\, dt$$

$$y_e = y_e(0) + \int_0^t v_{ee}\, dt$$

$$z_e = z_e(0) + \int_0^t w_{ee}\, dt$$

The aircraft's altitude is:

$$h = - z_e$$

The equations given in this Section can be simplified in several ways having practical interest, e.g. by linearizing (8-4) and (8-2) and/or by restricting some or all of the angles ψ, ψ_w, θ and φ to small values. Further analysis along such lines is felt, however, to be somewhat beyond the scope of this report.

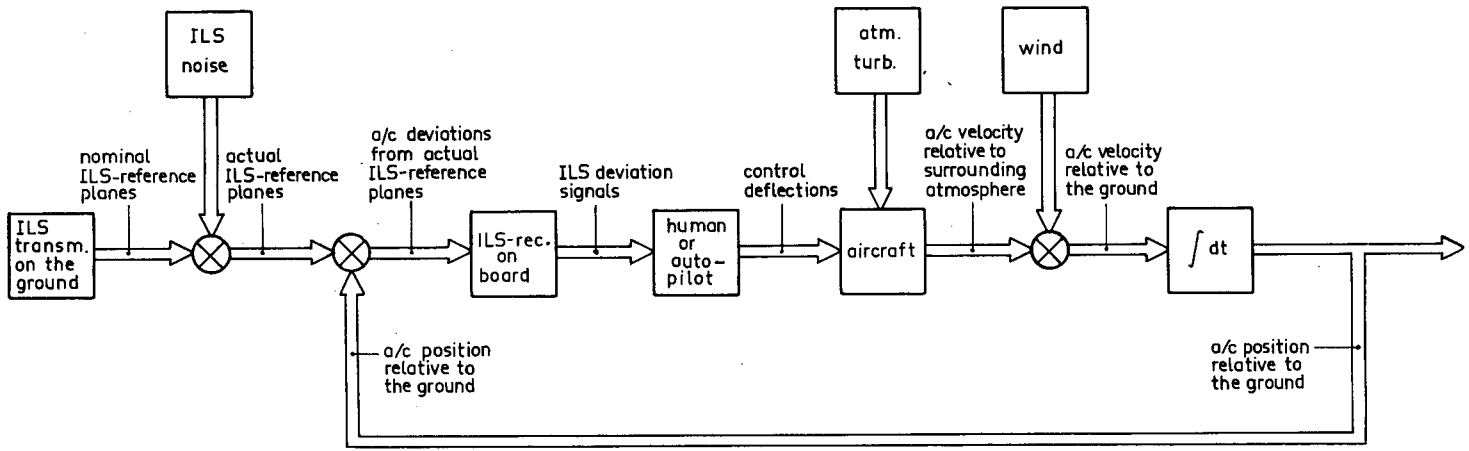

Fig. 1: External disturbances acting on an aircraft during approach and landing.

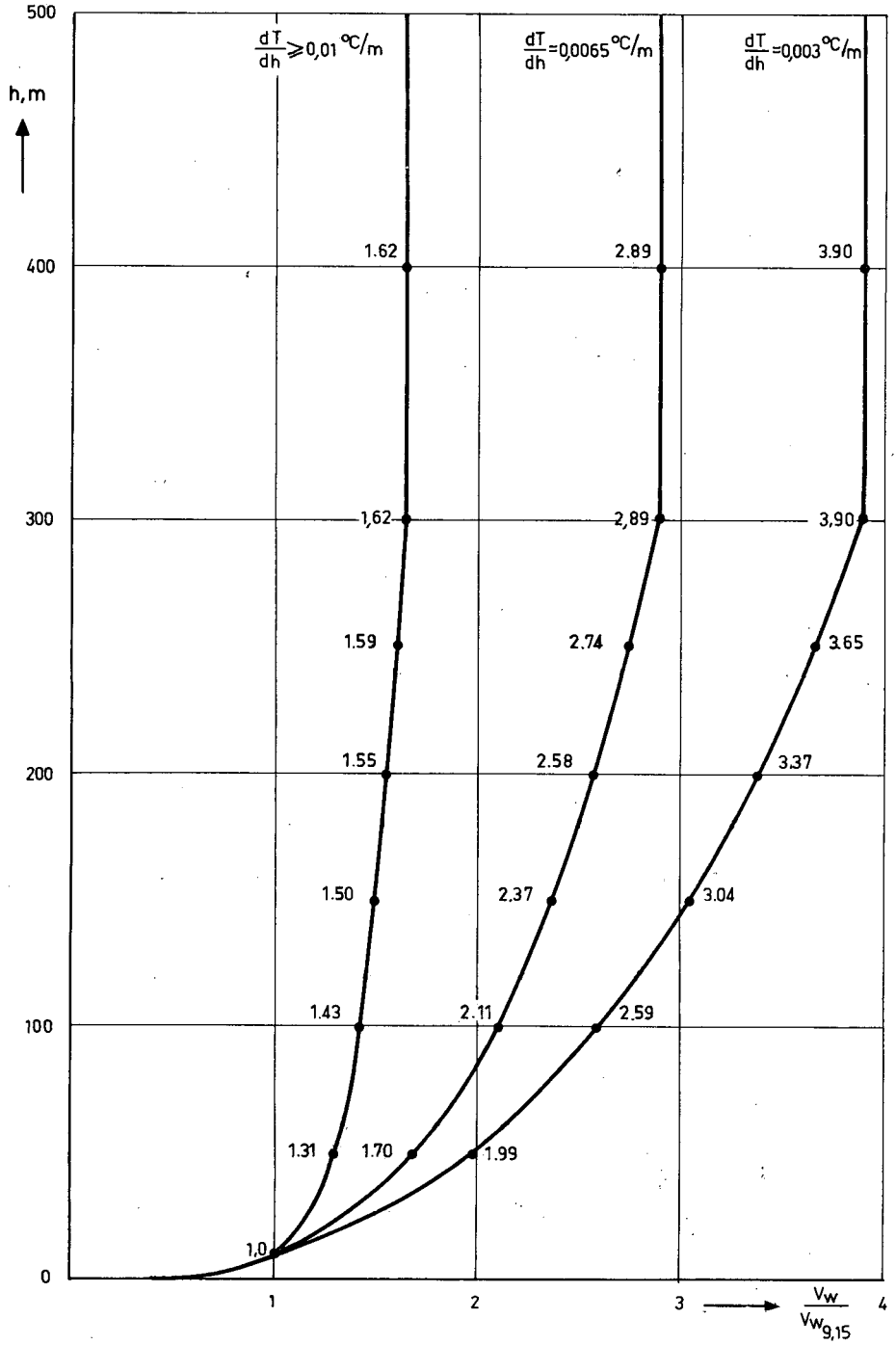

Fig. 2: Wind profiles for three stability conditions of the atmosphere.

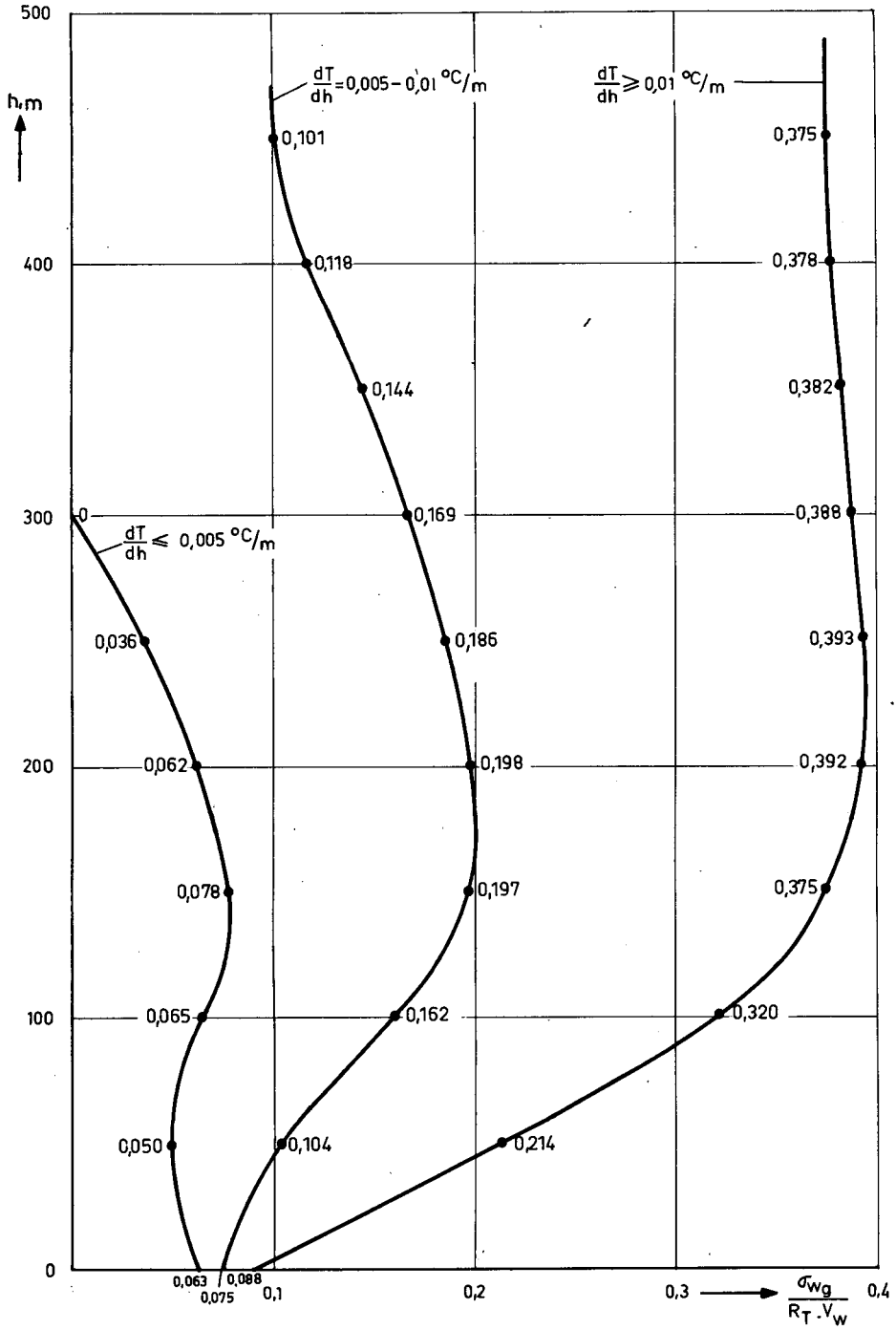

Fig. 3: Standard deviation of vertical gust velocity as a function of altitude.

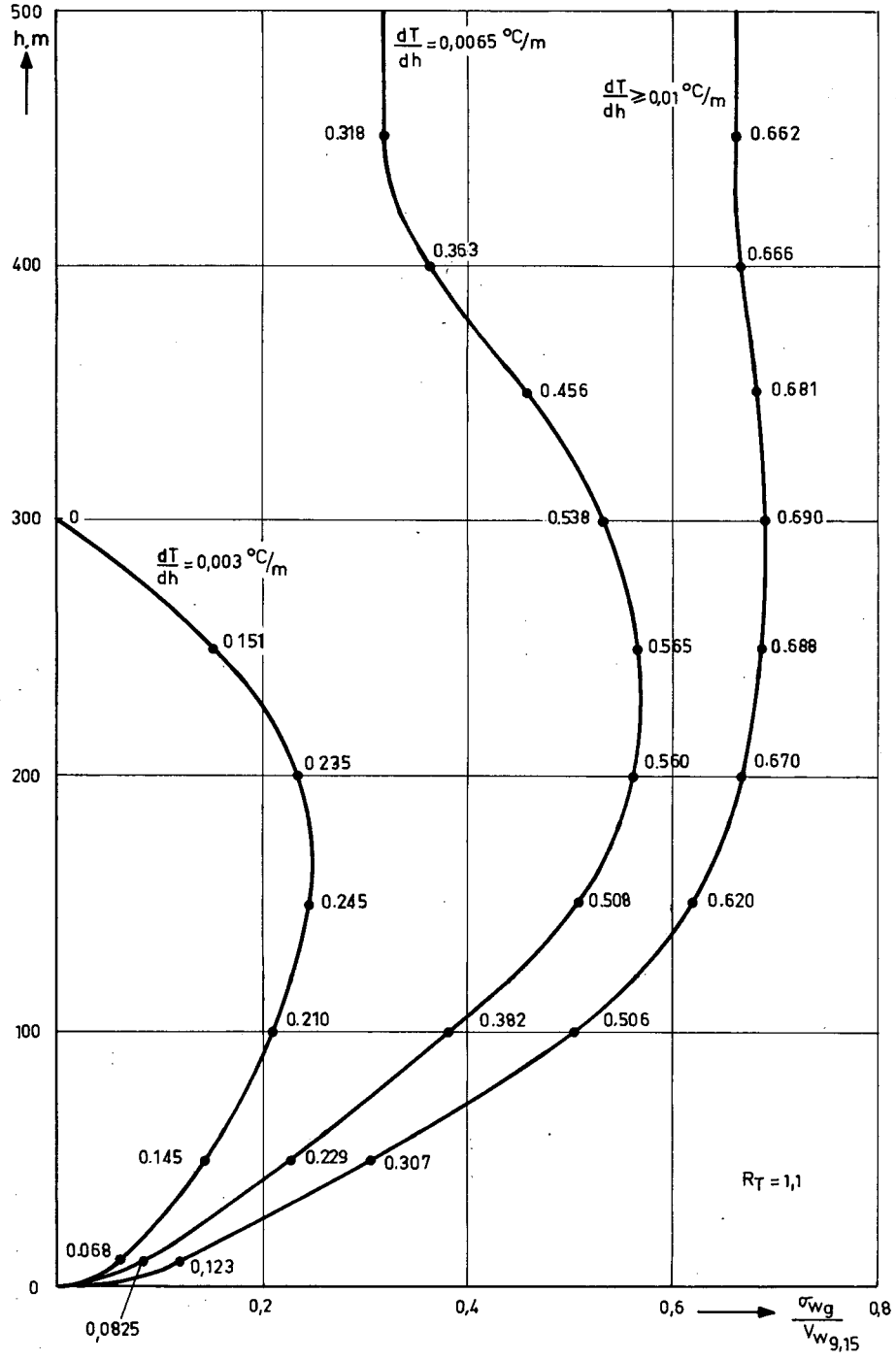

Fig.4: Standard deviation of vertical gust velocity as a function of altitude.

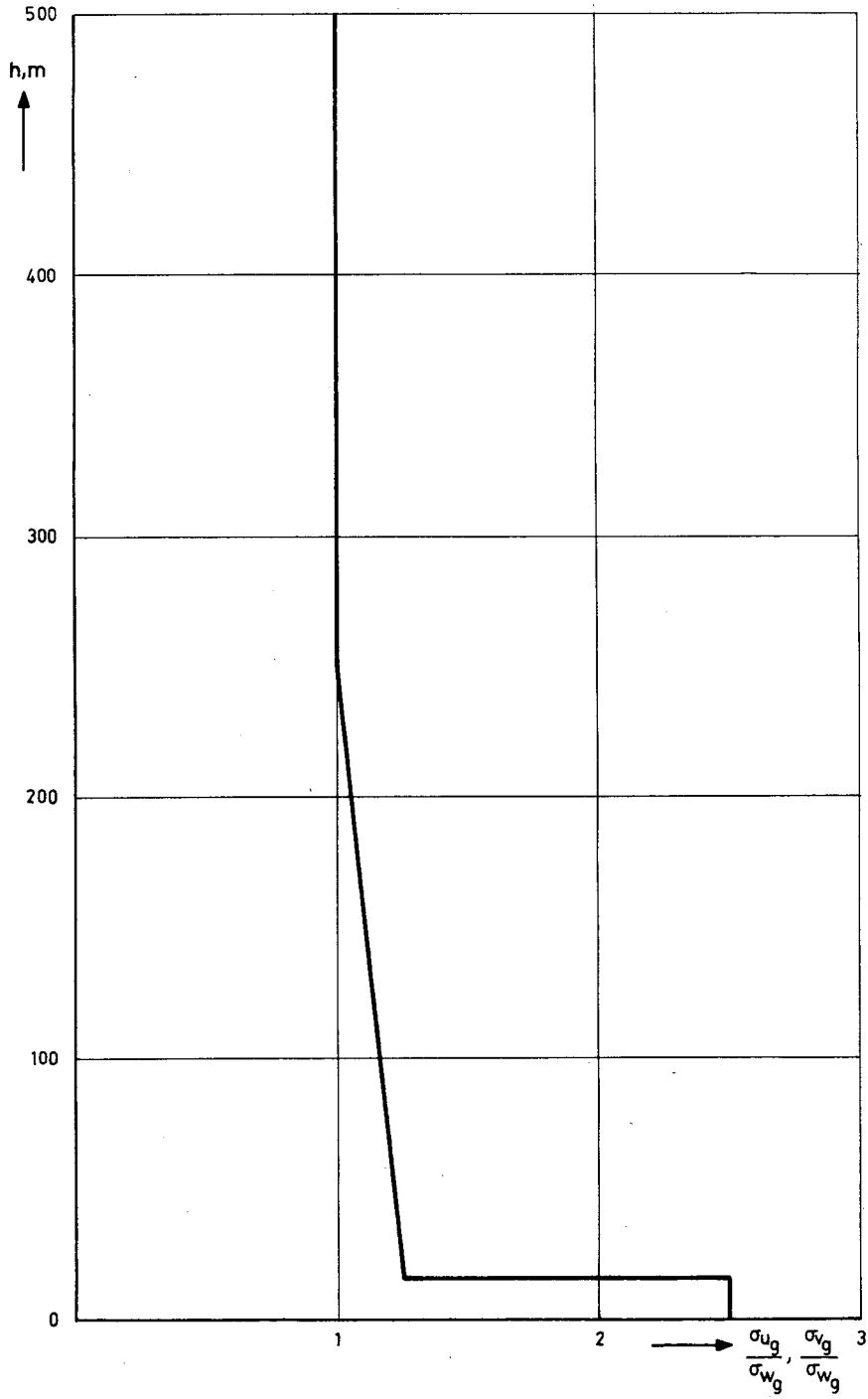

Fig. 5: Ratios of standard deviations of gust velocities as a function of altitude.

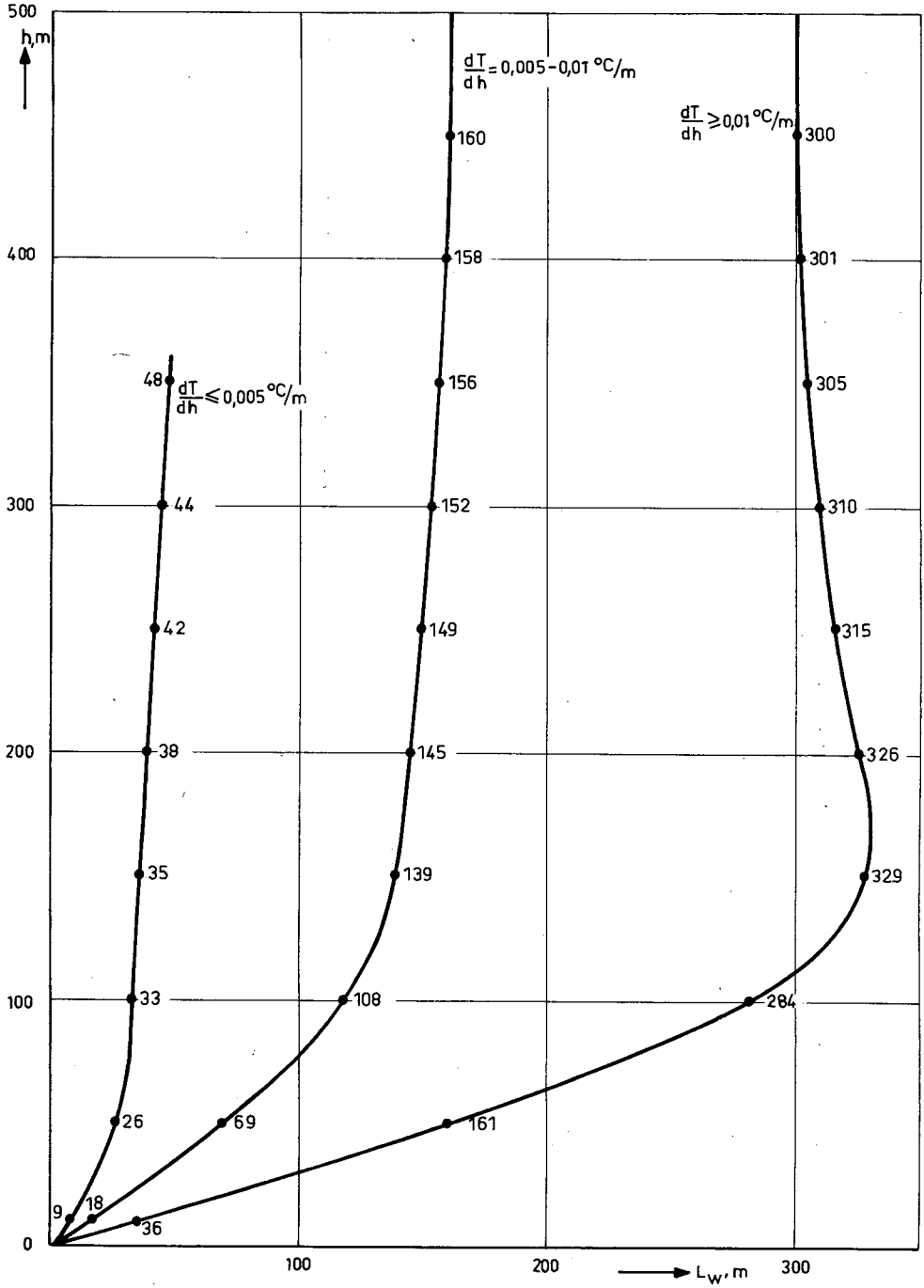

Fig. 6: Scale of vertical turbulence as a function of altitude.

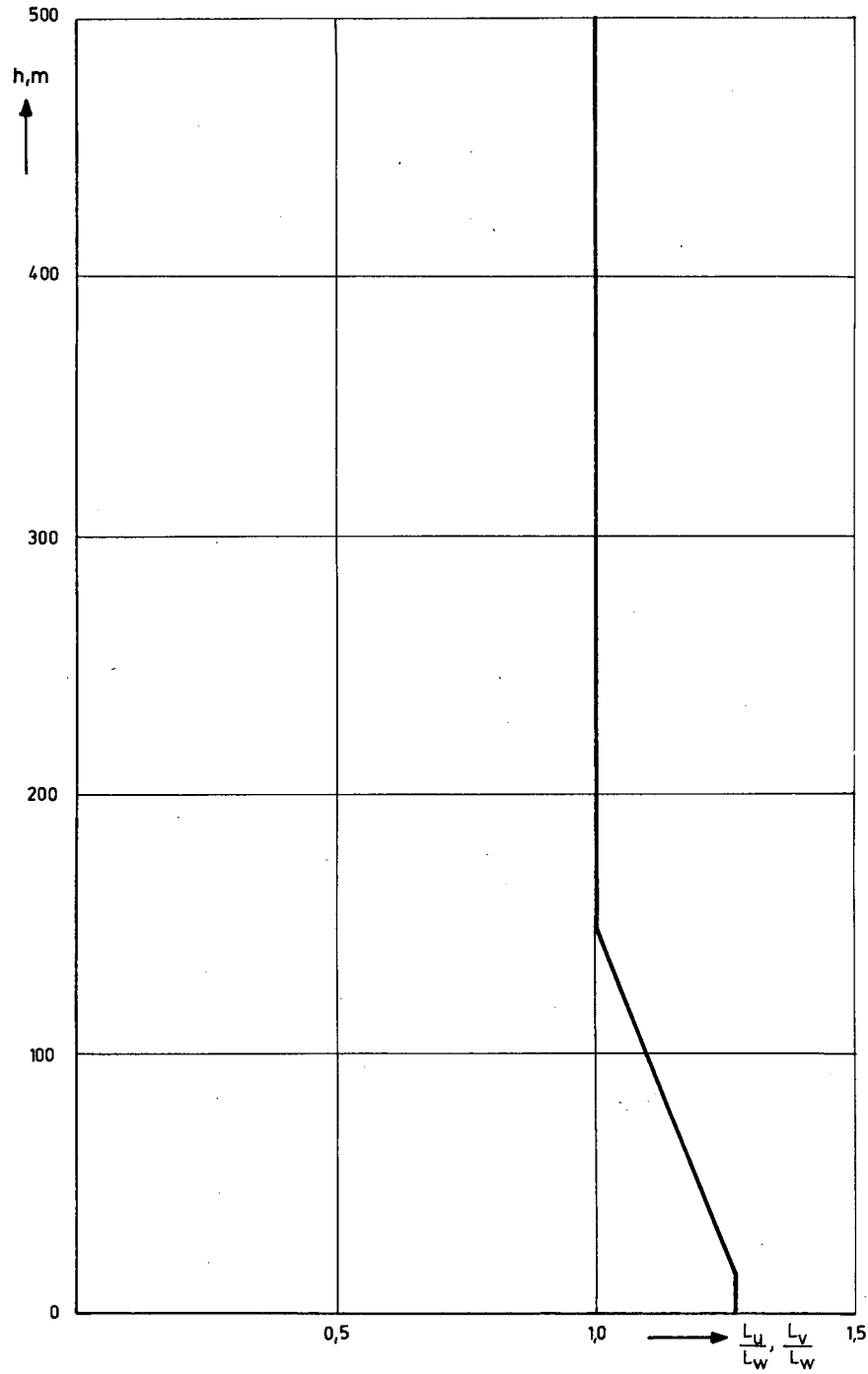

Fig. 7: Ratios of scales of turbulence as a function of altitude.

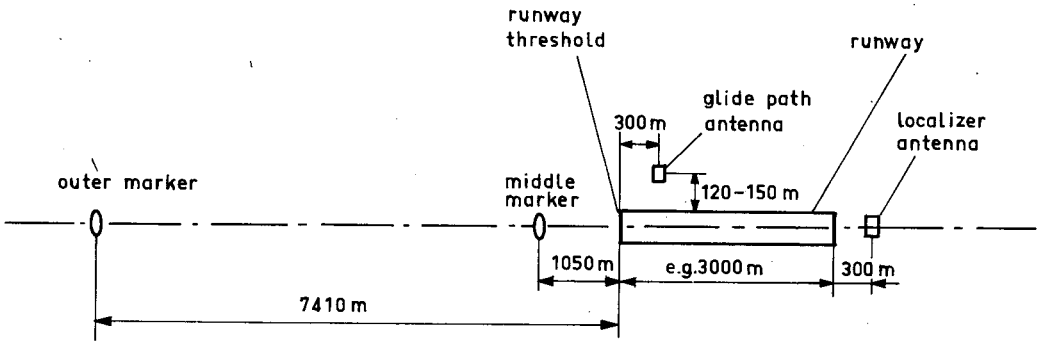

Fig.8: Typical ILS installation.

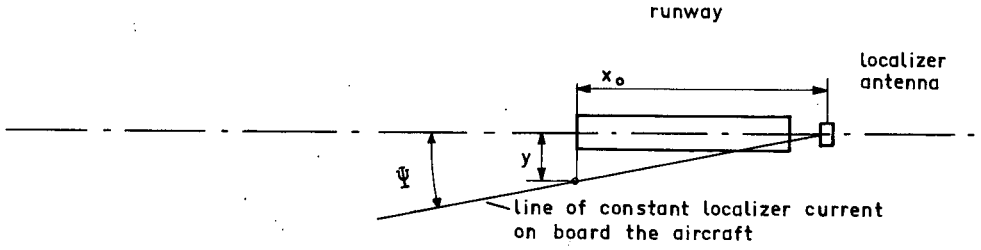

Fig.9: Radiation pattern of the localizer antenna.

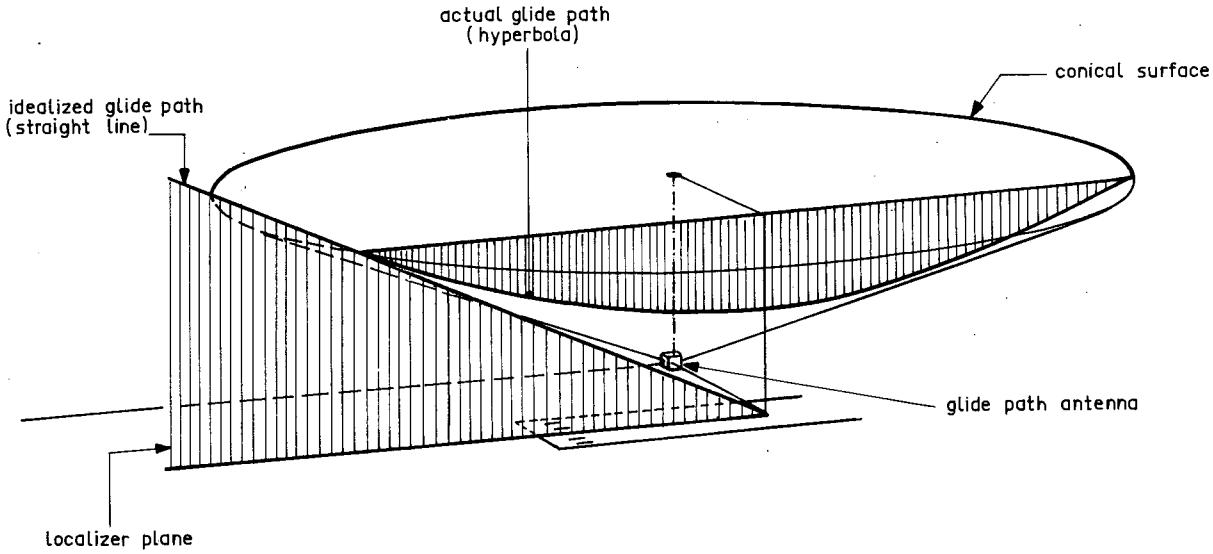

Fig.10: Radiation pattern of the glide path antenna.

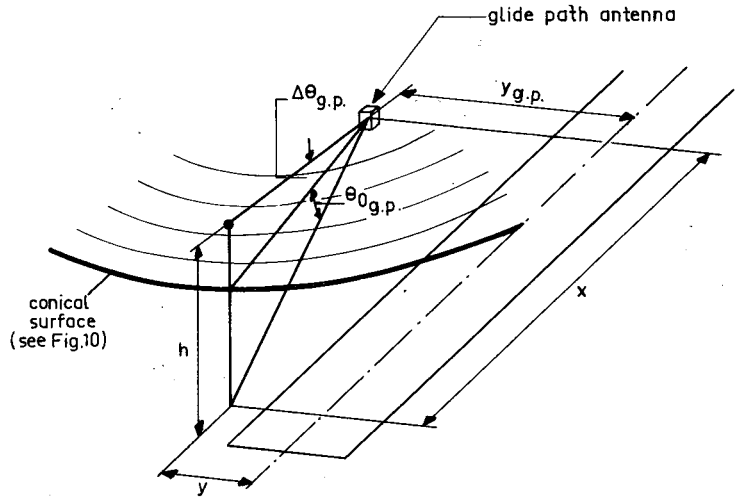

Fig. 11: The definition of glide path error $\Delta\theta_{g.p.}$

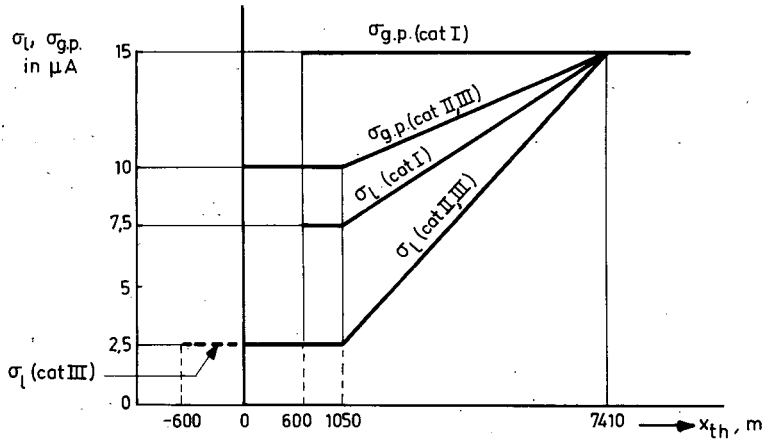

Fig. 12: Maximum allowable ILS-localizer and glide path noise.

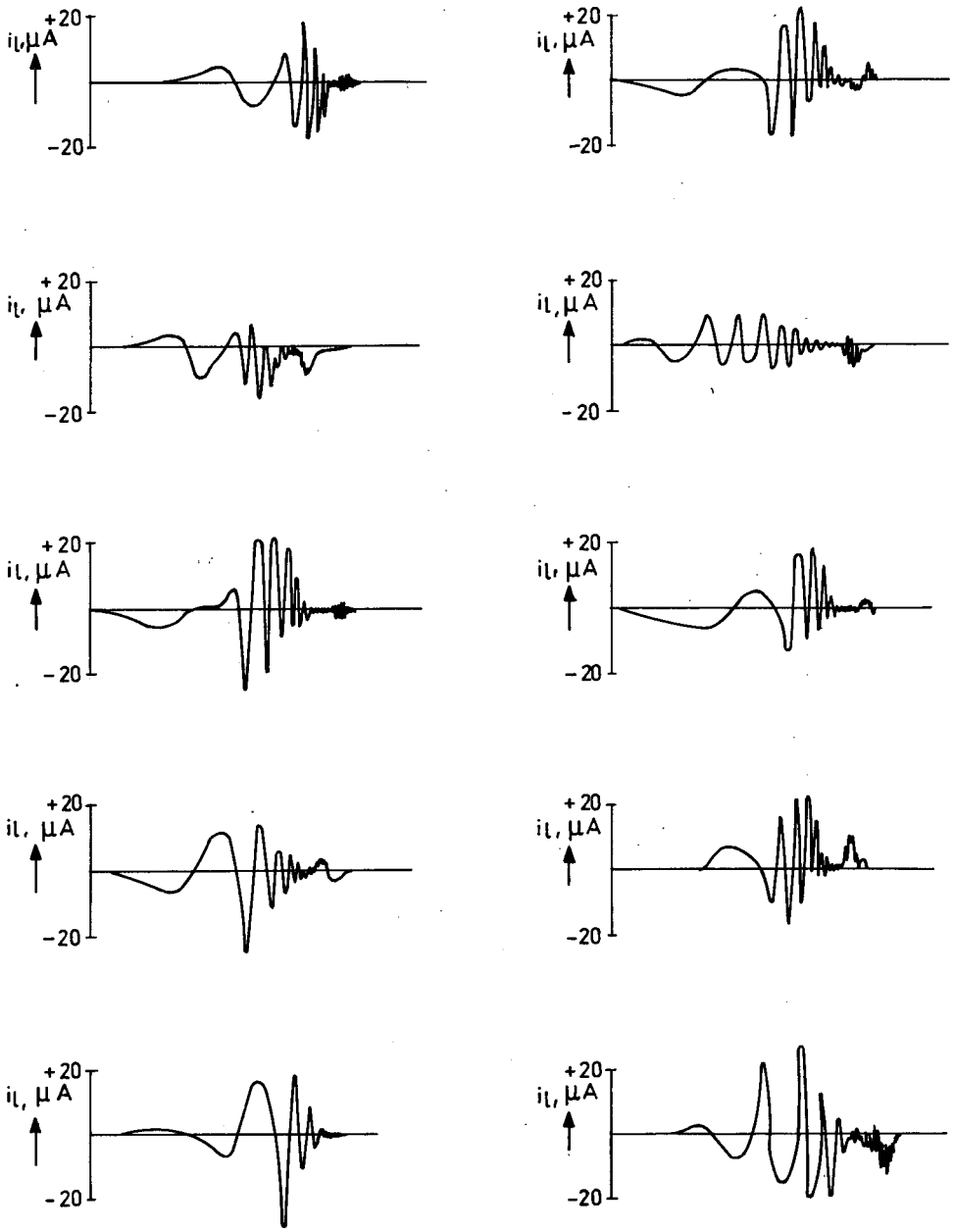

Fig. 13: Some typical interferences on the localizer current due to an overflying aircraft (Ref. 12).

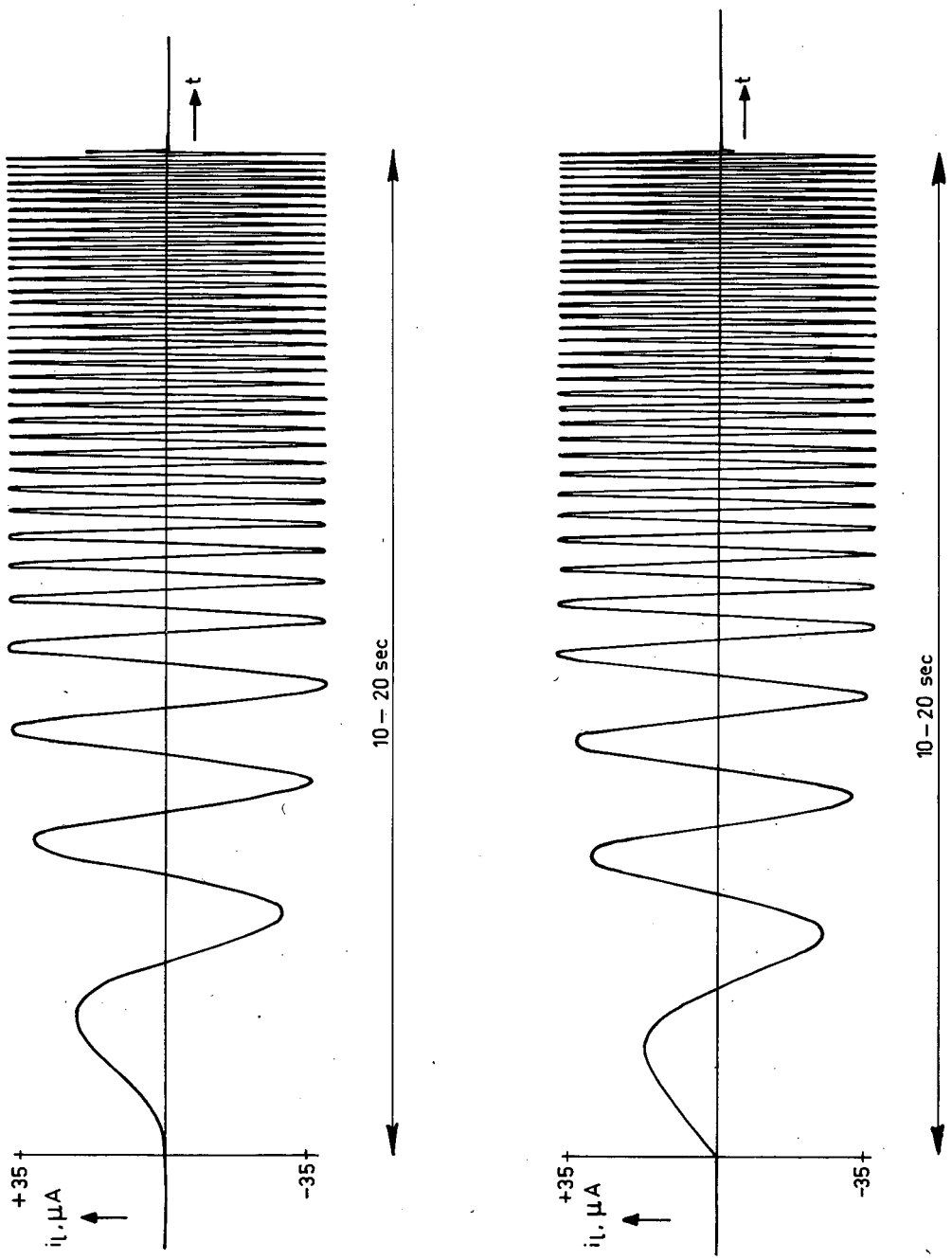

Fig.14: Simulated interferences due to an overflying aircraft, as proposed in (Ref 12).

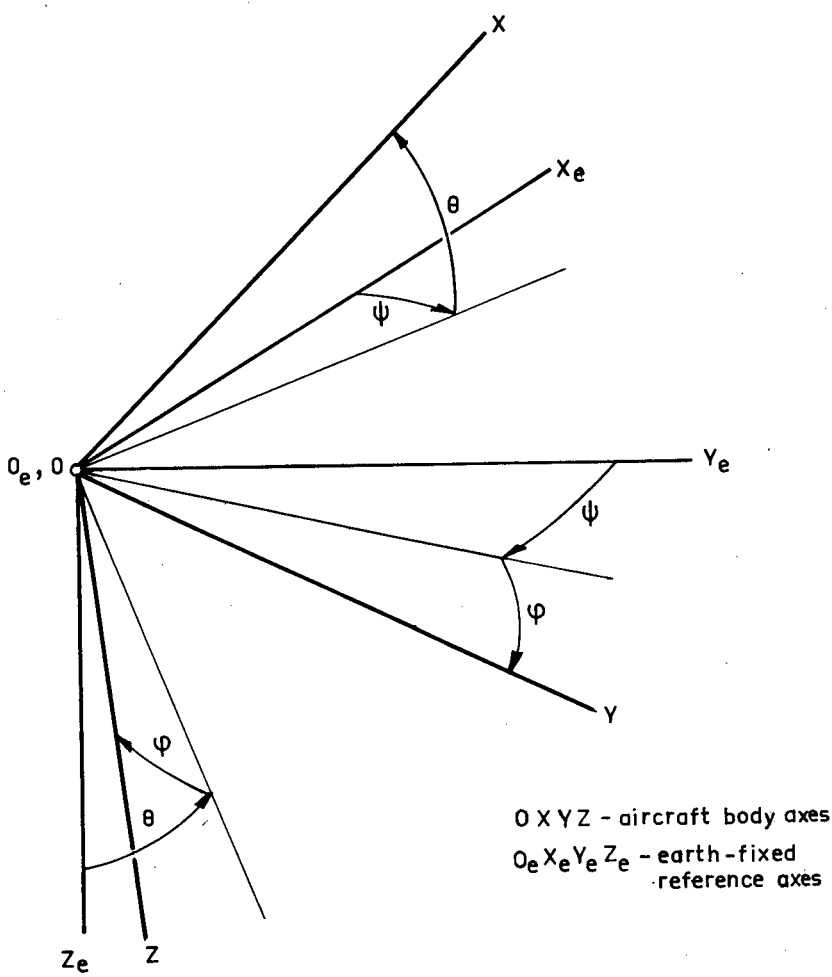

Fig. 15: Aircraft attitude defined by the angles ψ, θ, φ

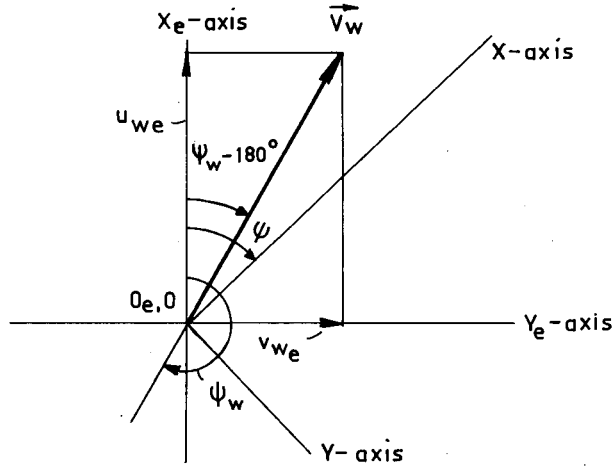

Fig.16 : The wind velocity vector $\vec{V}_w$ and its components u_{we}, v_{we}